AWARD/ MODIFICATION

3a. ISSUED BY:
Office of Naval Research
875 North Randolph Street
Arlington, VA 22203-1995

1. INSTRUMENT TYPE: Grant
3b. CFDA: 12.300
2. AUTHORITY: 10 USC 2358, 31 USC 6304
3c. DUNS NUMBER:

4. AWARD NO.	5. MODIFICATION NO.	6. MODIFICATION TYPE	7. PR NO.
N00014-13-1-0393		New	13PR04983-00

8. ACTIVITY/AGENCY PROPOSAL NO.	9. RECIPIENT PROPOSAL NO.	10. PROPOSAL DATE	11. ACTIVITY TYPE	12. PROGRAM TYPE
N/A	N/A	11-JAN-13		onr

13. ISSUED TO
13a. ADDRESS:
UNIVERSITY OF TEXAS AT ARLINGTON
OFFICE OF SPONSORED PROJECTS
PO BOX 19145
ARLINGTON, TX 76019-0145

13b. CAGE: 2N798
13c. EDI/EFT NUMBER: 5131AV

14. REMITTANCE ADDRESS (IF DIFFERENT FROM BLOCK 13):
Same as block #13

13d. BUSINESS OFFICE CONTACT: JEREMY FORSBERG
13e. TELEPHONE NUMBER: (817) 2722105
13f. EMAIL ADDRESS: j.forsberg@uta.edu

15. RESEARCH TITLE AND/OR DESCRIPTION OF PROJECT AND/OR PROPOSAL TITLE:
Influence of High Pulsed and Continuous Magnetic Fields on the Corrosion and Microstructure of Metallic Conductors

16. FUNDING	ACTIVITY/AGENCY SHARE	RECIPIENT SHARE	TOTAL
PREVIOUSLY OBLIGATED:	$.00	$.00	$.00
OBLIGATED BY THIS ACTION:	$25,000.00	$.00	$25,000.00
TOTAL OBLIGATED ON AWARD:	$25,000.00	$.00	$25,000.00
FUTURE FUNDING:	$.00	$.00	$.00
GRANT TOTAL:	$25,000.00	$.00	$25,000.00

17. CURRENT FUNDING PERIOD
N/A THROUGH N/A

18. PERIOD OF PERFORMANCE
01-FEB-13 THROUGH 31-JAN-14

19. ACCOUNTING AND APPROPRIATION DATA:
See attached Financial Accounting Data Sheet (s)

20a. PRINCIPAL INVESTIGATOR/RECIPIENT TECHNICAL REPRESENTATIVE:
DAVID ALAN WETZ
20b. TELEPHONE NUMBER: () 8172721058
20c. EMAIL ADDRESS: wetz@uta.edu

21. TECHNICAL REPRESENTATIVE
21a. NAME: Eric Wuchina
21b. CODE: ONR 332
21c. ADDRESS:
Office of Naval Research
875 North Randolph Street
Arlington, VA 22203-1995
21d. TELEPHONE NUMBER: 703 696-4409
21e. EMAIL ADDRESS: WUCHINE@ONR.NAVY.MIL

22. AWARDING OFFICE CONTACT
22a. NAME: Elizabeth Ford
22b. CODE: ONR BD025
22c. ADDRESS:
Office of Naval Research
875 North Randolph Street
Arlington, VA 22203-1995
22d. TELEPHONE NUMBER: (703) 696-2576
22e. EMAIL ADDRESS: FORDE@ONR.NAVY.MIL

23a. ADMINISTRATIVE OFFICE:
ONR REG SAN DIEGO-N66018
140 SYLVESTER ROAD
BLDG 140 ROOM 218
SAN DIEGO, CA 92106-3521
PHONE: (619) 221-5490
FAX: (619) 221-5615
23b. CODE: N66018

24. SUBMIT PAYMENT REQUEST TO:
Same as block #23a

25a. PAYING OFFICE:
DFAS COLUMB-NAVY ACQ HQ0251
COLUMBUS, OH 43213
25b. CODE: HQ0251

26a. PATENT OFFICE:
Office of Naval Research
ATTN: ONR BDCC
One Liberty Center
875 North Randolph Street, Suite 1425
Arlington, VA 22203-1995
26b. CODE: N00014

AWARD NO. N00014-13-1-0393	**AWARD/MODIFICATION**	MODIFICATION NO.	

27. SPECIAL INSTRUCTIONS:

28. DELEGATIONS: The administration duties listed below have been delegated to the administrative office (block 23a). Upon request the awarding office contact (block 22) will make their full text eveilable. Please direct questions to the contects @: http://www.onr.navy.mil/Contracts-Grants/Regional-Contacts.aspx

Full Delegation

29. TERMS AND CONDITIONS: The following terms and conditions ere incorporated herein by reference with the same force and effect as if they were given in full text. Upon request the awarding office contact named in block 22 will make their full text available, or they can be found as described below.

DOCUMENT

The following documents may be found at:
http://www.onr.navy.mil/Contracts-Grants/submit-proposal/grants-proposal/grants-terms-conditions.aspx

UAAC Acceptance C November 2003
Agency Specific February 2011
UAWA Award A November 2003
Core June 2011

30. OPTIONS OPTION NO. AMOUNT PERIOD
(1)
(2)
(3)
(4)

31. REPORTS: The following reports must be submitted to the indicated addressees, in the indicated quentities, within 90 days following the expiration or termination of the project. Final Technicel Reports must have a SF298, Report Documentation Page, eccompanying them. Unless otherwise stated in the ewerd/modification, complete Block 12e of the SF298 as follows: "Approved for Public Releese; distribution is Unlimited".

ADDRESSEE	REPORT TYPE	COPIES
See block #21	Final Technical Report with SF298 Interim Research Performance Report (As Required) with SF298	1 1
See block #23a	Report of Inventions and Subcontracts - DD 882 Final Technical Report Interim Research Performance Report (As Required) Final Federal Financial Status Report - SF425 - Including Line Item 11	1 1 1 1
Defense Technical Information Center 8725 John J Kingman Road Ste 0944 Fort Belvoir, VA 22060-6218	Final Technical Report with SF298 Interim Research Performance Report (As Required) with SF298	1 1
See block #26a	Report of Inventions and Subcontracts - DD 882	1
Naval Research Laboratory ATTN: CODE 5596 4555 Overlook Avenue SW Washington, DC 20375-5320	Final Technical Report Interim Research Performance Report (As Required) with SF298	1 1

32. FOR THE RECIPIENT		33. FOR THE UNITED STATES OF AMERICA	
32a. SIGNATURE OF PERSON AUTHORIZED TO SIGN N/A - SIGNATURE NOT REQUIRED ON THIS AWARD		33a. SIGNATURE OF AWARDING OFFICER Elizabeth Ford	
32b. NAME AND TITLE OF SIGNER	32c. DATE SIGNED	33b. NAME AND TITLE OF AWARD OFFICER Elizabeth Ford	33c. DATE SIGNED 30-JAN-13

ONR AWARD FORM (10/99) - version 1 1

Final Report

Influence of High Pulsed and Continuous Magnetic Fields on the Corrosion and Microstructure of Metallic Conductors

Submitted to:

Dr. Eric Wuchina
eric.wuchina@navy.mil

Grant Number N00014-13-1-0393

Performance Period: February 1, 2013 – March 31, 2014

Submitted by:
David Alan Wetz Jr., Ph.D
Assistant Professor
University of Texas at Arlington
College of Engineering
Electrical Engineering Department
416 Yates Street
537 Nedderman Hall
Arlington, Texas 76019-0016
Phone: (817) 272-1058

Abstract

Corrosion is among the most costly and severe maintenance problems the US Navy faces on a daily basis. As the US Navy works towards fielding an all-electric ship, it is unclear how the corrosion rate of its structural and current conducting alloys will be impacted when they are repeatedly exposed to the high continuous magnetic fields from external and self-induced sources. The high currents that propel the ship and other complex electrical loads induce these magnetic fields. Experimental results collected from exposure of four engineering alloys to continuous magnetic fields and high-pulsed currents will be presented. The materials tested include 304 stainless steel, 416 stainless steel, 1018 steel, and 8620 steel as these offer structural integrity as well as both magnetic and nonmagnetic properties. A 3.5% NaCl aqueous solution is employed as the electrolyte for all experiments. Samples have been exposed to a continuous 0.45 T magnetic field generated by a DC electromagnet, and by a high-pulsed current from a capacitive pulsed power supply sinking up to 9000 A, respectively. Potential vs. time, anodic polarization, and linear polarization experiments have been conducted to measure and understand the kinetics behind the corrosion process along with the possible impact of the magnetic fields. After the Potential vs. Time experiments, SEM examinations have been conducted to compare baseline samples not exposed to magnetic fields to those, which have been exposed to magnetic fields and to those exposed to high-pulsed currents. The experimental setups and the results of the experiments performed thus far will be discussed.

Introduction

The US Navy's near term plans involve integration of electric propulsion and weapon systems into their fleet. These electrical architectures and complex loads require significant current, as high as a few Mega-Amperes in some cases, to be sourced. In some applications, high currents will flow continuously, for example when continuous DC or AC loads are operated. The conduction of a time varying current leads to the generation of a magnetic field according to the Biot–Savart law. Anything located within close proximity to the current carrying conductors, including the conductors themselves, are exposed to the magnetic fields. While the primary conductors, which actually carry current to the loads, are most likely to be copper or aluminum, other engineering alloys may also be used in some specialty applications, especially in high current applications where high electromagnetic forces are created or structural support is needed. It is important to keep in mind that the alloys may not have magnetic properties themselves, which can alter the magnetic fields and their strength. When used in naval applications, the metals will be exposed to a natural sea weather environment, which causes destructive corrosion to the most active materials. The degree to which they will be exposed to harsh environments will vary of course and while much is already done to prevent corrosion in forward operating bases (FOBs) and aboard Naval ships, it is unclear to what degree the high magnetic fields will affect the extent of corrosion in these metallic alloys. The research being documented here is being performed to better understand the impact magnetic fields may have on the corrosion process of various metallic alloys. Through the results obtained, which will be presented later, it has been found that high magnetic fields do impact both the corrosion

potential and the corrosion rate of untreated materials such as 304 stainless steel, 416 stainless steel, 1018 steel, 8620 steel. It is believed that the magnetic field influences the corrosion process by affecting the oxygen concentration at the surface of the anode.
Only recently, others have conducted research aimed at investigating how high continuous magnetic fields impact the rate of corrosion of metallic alloys [1-9]. As indicated previously, there are an extremely wide variety of different loads, which must be powered aboard future naval vessels in the harsh sea environment. These range anywhere from high-energy weapons, which may require high pulsed currents on the order of several Mega-Amperes, therefore it is critical that the effects of magnetic fields on the corrosion rate of the conducting and structural alloys be well understood. Due to corrosion's annual cost worldwide of $2.2 trillion dollars, governments and structural industries are looking into any and all means, which may reduce replacement and maintenance costs by understanding the corrosion process and protecting the alloys used [10]. In this particular study, alloys of interest are being experimentally exposed to continuous magnetic fields and high-pulsed currents.

Utilizing the support from the ONR Grant documented here, two novel experimental setups have been designed and built to better understand the influence the external magnetic fields and high-pulsed current effect corrosion. Both test cells had constraints that made using commercial off the shelf (COTS) electrochemical test setups difficult to use. The first setup had to be designed to fit tightly in between a pair of electromagnet poles. To account for this tight fit a 1000 mL beaker was used to keep the electromagnet poles as close as possible, allowing for higher magnetic field strengths near the sample. The other experiment required the sample to pierce through the test cell, so that current could be passed through the sample while electrically connected to the source.

The experimental setup, seen in Figure 1(left), utilizes a DC driven electromagnet and a 1000 mL glass beaker with a custom made PTFE lid. The lid is used to support the purge tube as well as the reference, counter, and working electrodes. Prior to testing, the beaker is filled with 800 mL of 3.5% NaCl aqueous solution. Using a Saturated Calomel Electrode (SCE) as a reference and a graphite counter electrode, potential vs. time and anodic polarization measurements were conducted to evaluate the corrosion behavior under the application of the magnetic field. It should be noted that the samples were not treated for corrosion prevention prior to testing. When baseline measurements are made, the same setup is used but testing is conducted away from the electromagnet. Using the electromagnet, the field lines are nearly uniform through the entire test sample. The adjustable 0 – 70 ADC field winding current enables the magnetic field to vary from roughly 0 T to 0.5 T, as seen in Figure 1(right). The current testing setup configures the sample parallel to the magnetic field. The counter electrode is off set from the sample.

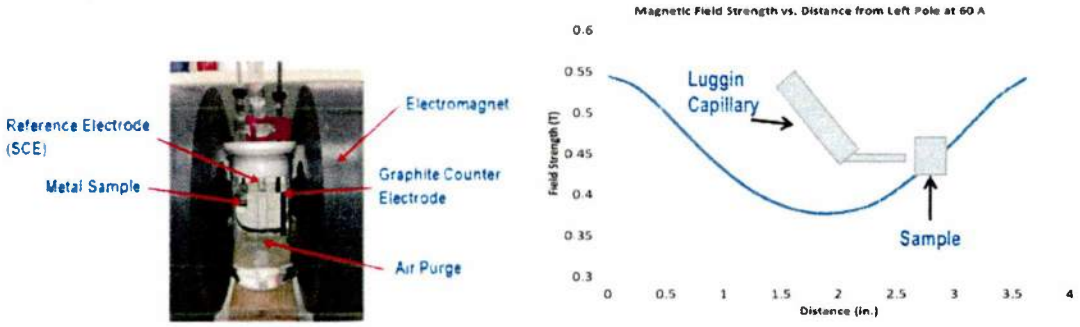

Figure 1. (left) Electrochemical test cell located within a DC electromagnet which applies a uniform magnetic field across the sample and (right) plot of field strength vs. position when the electromagnet current is 70 ADC.

All test samples were cross-sectioned from 1 cm diameter rods. Following cutting, the samples were mounted in epoxy, then rough ground and polished with 1000 grit paper as the last step. Lastly the samples were fine polished using a 0.1 micron alumina paste. Figure 2 presents a typical sample after polishing.

Figure 2. Polished 1018 steel sample.

The second experimental setup is configured such that high-pulsed currents, on the order of a few kilo-Amperes, can be conducted through the sample. This generates a high-pulsed magnetic field, which is wrapped around the sample according to the right hand rule. This setup is shown in Figure 3(left). The current is sourced by a 63 kJ, 450 V capacitive pulsed power supply which is made up of eighteen independently controllable 35 mF electrolytic capacitor modules. The critically damped RLC output pulse has a full width half maximum (FWHM) width of roughly 4 ms. The rod samples are prepared in the same method as that discussed above, beginning with a wet rough grind and finishing with the 0.1 micron alumina paste. After the rod samples are prepared, it is clamped into the copper bus work using custom copper clamps. It should be noted that the rod samples used in this setup have a diameter of 0.064 cm (0.25 in) rather than 0.953 cm as used in the first experimental setup. This is done to ensure that the skin effect does not play a dominant role in the current distribution.

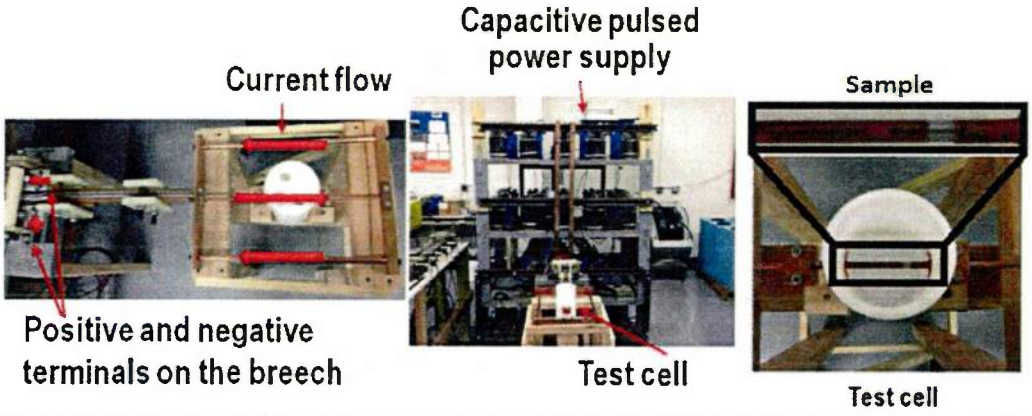

Figure 3. Electrochemical test cell connected to a pulsed power supply (left), which is used to apply a pulsed current/magnetic field (middle) to the sample under test (right).

As seen in the photographs of the setup, the rod sample is passed through a custom made PTFE beaker which holds 800 ml of 3.5% NaCl solution. Current flows through the rod sample and returns to the supply in two parallel paths ensuring an equal distribution in the forces induced from current flow in opposite directions. One issue of concern is the increased surface area exposed to the electrolyte since the rod samples are longer in this setup. In order to expose the same sample surface area to the solution, significant portions of the surface are initially covered using polyimide, Kapton, tape. In order to prevent electrolyte from leaking outside the test cell, high temperature RTV is used to seal around any openings in the beaker. One last consideration worth discussing is the ohmic heating of the rod sample due to high current flow. Since the electrolyte is liquid based, it is desirable to maintain the sample surface temperature below 100°C, the boiling temp of water. Rod samples were initially pulsed in an open-air environment with increasing currents and an insulated thermocouple mounted on the surface. From that, the peak currents were measured which limit the surface temperature below 100°C.

Experimental Results

The present experiments were aimed at characterizing the impact of a magnetic field on the corrosion behavior of the selected alloys, namely, 304 austenitic stainless steel, 416 stainless steel, 1018 steel, and 8620 steel. The properties of these alloys vary considerably as shown in Table 1. In the first set of experiments, each alloy sample was immersed in 800 mL of 3.5% NaCl solution and experiments were performed with and without the presence of a magnetic field generated by the electromagnet. Note from Figure 1(right), that the magnetic field strength at the surface of the metal is roughly 0.45 T. The open circuit potential (OCP) was recorded for about three hours until it stabilized. Figure 3, shows the potential vs. time measurements for all samples tested with and without the presence of the magnetic field. The results show that the magnetic field has no effect on the corrosion potential of 304 stainless steel and a very small effect (if any) on 416 stainless steel. On the contrary, the presence of the magnetic field resulted in a significant reduction in the OCP of both 1018 and 8620 carbon steels. This clearly indicates that the magnetic

field moved the corrosion potential of these two materials in the active direction. The difference can be attributed to the presence of Chromium in the two stainless steels tested and their ability to passivate. On the other hand, 1018 and 8620 remain always in the active region and simply the application of the magnetic field intensifies the activity.

Table 1. Datasheet material properties of 304 stainless steel, 416 stainless steel, 1018 steel, and 8620 steel [11].

Material	Permeability (H/m)	Resistivity (μohm-cm)	Density (g/cc)	Typical Hardness (Brinell)	Magnetic
304 SS	1.004	72	7.9	<=201	No
416 SS	700-1000	57	7.8	365	Yes
8620 Steel	529	2.34	7.85	183	Yes
1018 Steel	529	15.9	7.87	126	Yes

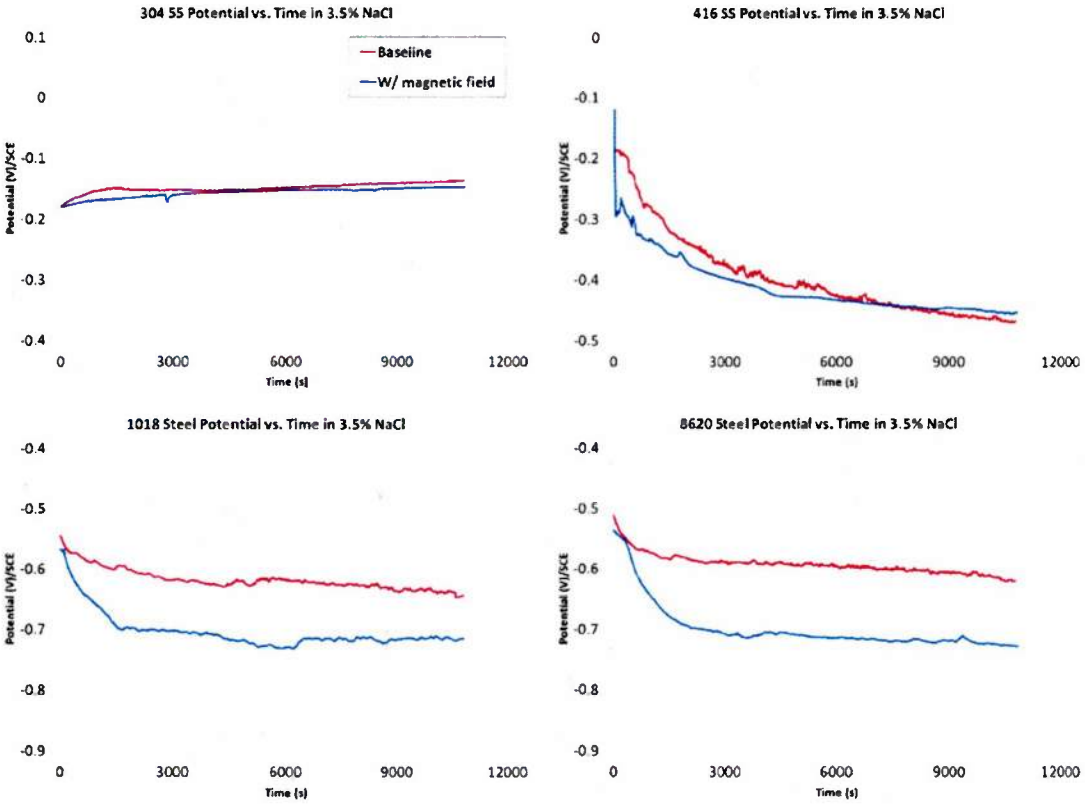

Figure 4. Corrosion potential of (top left) 304 SS, (top right) 416 SS, (bottom left) 1018 Steel, (bottom right) 8620 Steel with and without a .45 T magnetic field present in 3.5% NaCl.

It is important to note that 304 stainless steel is not magnetic but it passivates readily. This demonstrates that there is a relationship between the effects of the magnetic

field on corrosion and the magnetic properties of the alloy. It is believed that the magnetic nature of the alloy draws oxygen, which is paramagnetic, to the surface of the metal increasing the oxygen concentration at the surface thereby altering the rate of reactions and subsequently the corrosion potential. Note that the corrosion potential drops more steeply and stabilizes quicker when the latter three materials are used since the oxygen concentration is quickly saturated at the surface.

Figure 4 shows macro and SEM scale images of the samples tested with and without exposure to the magnetic field. While the macro scale images of the 304 samples appear identical, there is a lower density of pitting observed on the sample, which has been subjected to the magnetic field. The depth of the pits is very similar between the two 304 stainless steel samples. The variation observed from the other alloys tested is more severe. The corrosion of the other ferromagnetic alloys occurs mainly along the edges when the magnetic field is applied. This is a good indication of the magnetic field affecting the oxygen concentration at the surface of the alloy. When the magnetic field is applied to the sample, the magnitude of the magnetic field is largest at the edges. The higher strength of the magnetic field attracts the paramagnetic oxygen ions to the edges increasing the cathodic reaction in those regions.

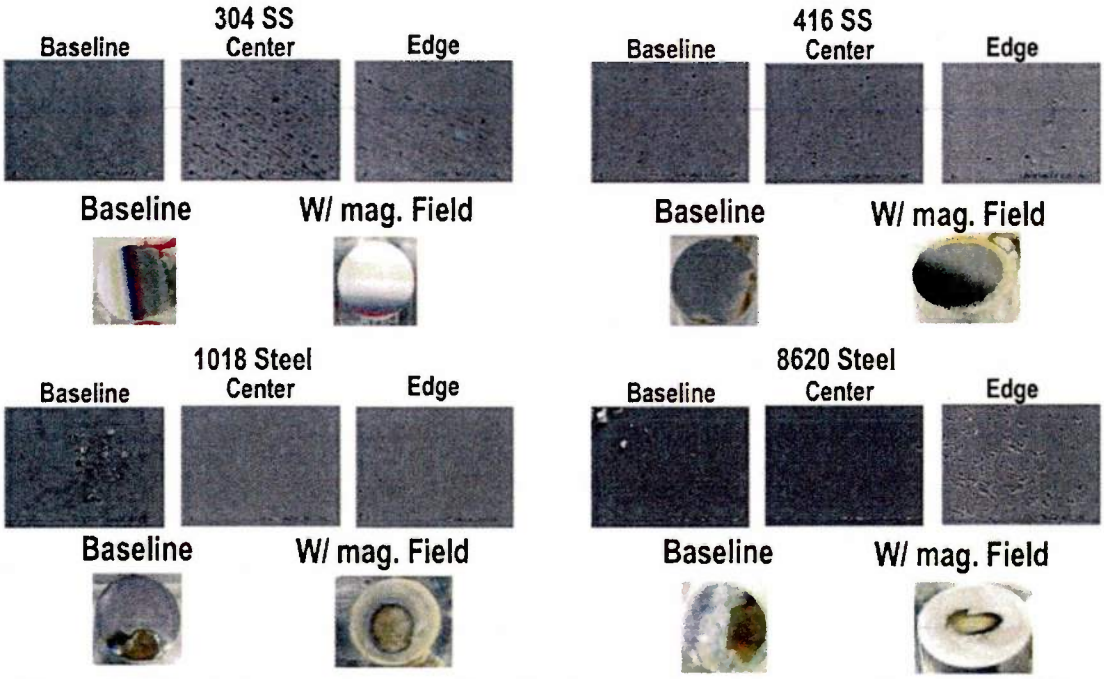

Figure 5. SEM and photographic images of both baseline samples and those exposed to magnetic fields, while they were immersed in 3.5% NaCl for three hours

The SEM images in Figure 5 provide a better understanding of how the magnetic field influences the location of the anodic reaction. After a magnetic field was applied to the 416 stainless steel, the center had a lower density and shallower pits than the baseline. The pits at the edge of the sample were present at a similar density but their depth was smaller when compared to those observed on the baseline sample. Both the 1018 steel and

8620 steel acted similar to one another when the magnetic field was applied. The center of the samples exposed to the magnetic field had similar pitting as that observed on the samples not exposed to the magnetic field. The edges of the samples exposed to the magnetic field have a higher pitting density and pitting depth when compared to the samples not exposed to a magnetic field. In short, the reaction rates and location of the reaction are dependent on the ferromagnetic properties of the alloys with the presence of an external magnetic field. It is important to remember that the 304 stainless steel sample was not affected by the external magnetic field.

Anodic polarization measurements were conducted to study the corrosion kinetics of the alloys. The experimental setup used here is the same as that used for the potential vs. time measurements however; a graphite rod is also introduced into the test cell. The ASTM G5 – 87 Standard was used as a template, and as per standard the test is started one-hour after immersion in the electrolyte. The experiment differentiated from the standard by leaving the test cell in open air instead of with an Argon purge. The magnetic field was applied while the sample was submersed in the electrolyte. The potential was scanned anodically at a rate of 1 mV/s. The corrosion rate was determined by Tafel extrapolation.

The results of the anodic polarization experiments are shown in Figure 5. The experiment is performed in an open-air environment similar to the potential vs. time experiment. The higher potentials are caused by the experiment initiated an hour after the test sample was placed in the electrolyte as per the ASTM G5 – 87 Standard. It should also be noticed that more noise was observed in the measurements conducted when the magnetic field was applied when compared with their baseline counterparts. The noise is believed to be introduced by the switch mode DC power supply used to drive the electromagnet.

The anodic polarization experiments of all four alloys indicate that the magnetic field causes activation and increases the corrosion current when compared to that measured in the baseline experiments. Table 2 summarizes the corrosion potentials and corrosion rates for all materials as determined from the anodic polarization experiments. The presence of the magnetic field was found to reduce the corrosion potential in all four materials and to cause higher active current densities. Even the 304 stainless steel and 416 stainless steel have been affected by the magnetic field. Both show somewhat lower corrosion potentials, higher anodic current densities and higher passive current densities. It is also interesting that 304 stainless steel shows a lower pitting potential in the presence of the magnetic field while 416 does not develop a clear passive region.

The effect of the magnetic field on the 1018 and 8620 steels is dramatic. The corrosion potential is shifted in the active region by 250 mV and the anodic current densities are increased by a couple of orders of magnitude. The paramagnetic nature of the oxygen ions can provide some reasoning for the observed behavior. However, there is not a clear understanding of these tremendous effects of the magnetic fields on the corrosion behavior. For example, the reduction of the pitting potential of 304 stainless steel and the higher passive current densities show that additional effects may be induced by the presence of the magnetic field.

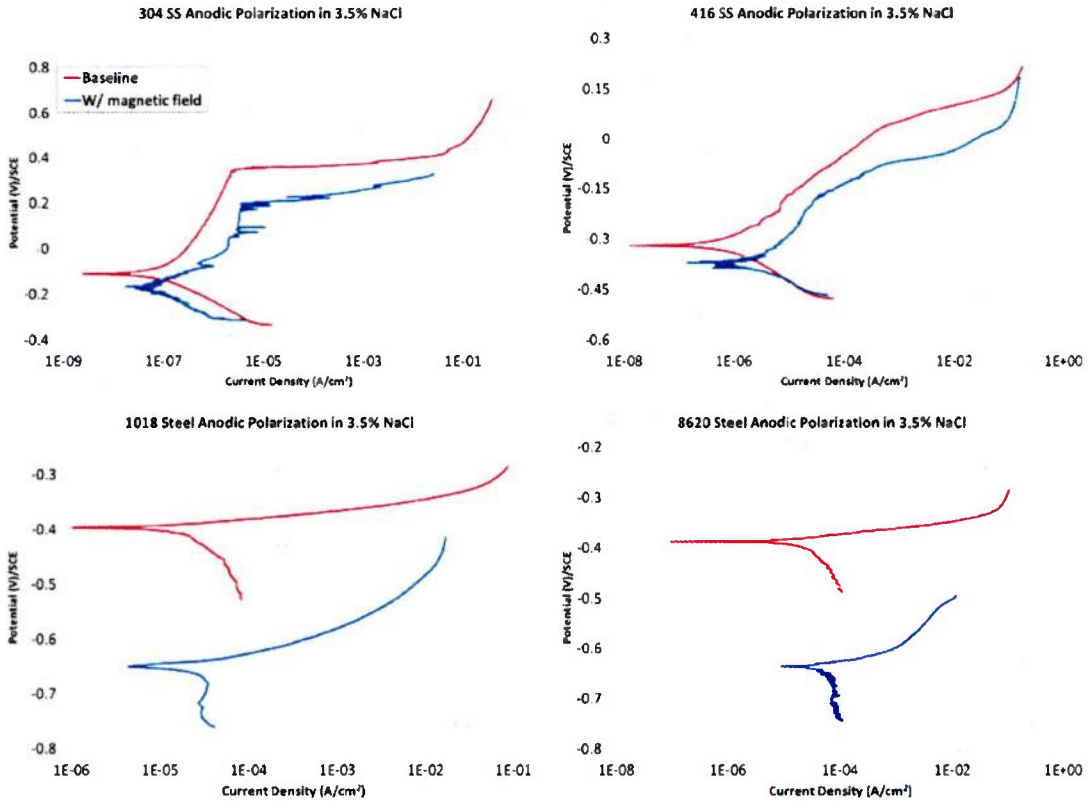

Figure 6. Anodic Polarization of (top left) 304 SS, (top right) 416 SS, (bottom left) 1018 Steel, (bottom right) 8620 Steel with and without a .45 T magnetic field present in 3.5% NaCl.

Table 2. Summary of the Corrosion Potential and Corrosion Rate under a Continuous DC Magnetic Field in 3.5% NaCl.

	Corrosion Potential, mV			Corrosion Rate, mA/cm^2		
Material	Baseline	W/ mag. field	ΔE	Baseline	W/ mag. field	Δ Change
304 SS	-112	-168	56	$6.81 * 10^{-5}$	$1.00 * 10^{-4}$	$-3.19 * 10^{-5}$
416 SS	-322	-371	49	$7.94 * 10^{-5}$	$2.72 * 10^{-3}$	$-1.93 * 10^{-3}$
1018 Steel	-397	-650	253	$1.92 * 10^{-2}$	$2.78 * 10^{-2}$	$-8.60 * 10^{-3}$
8620 Steel	-388	-636	248	$1.47 * 10^{-2}$	$6.1 * 10^{-2}$	$-4.64 * 10^{-2}$

In an effort to discern whether or not the hypothesis of oxygen attraction is correct, experiments were performed in which the electrolyte in the test cell was deareated using argon. These results are presented in Figure 7. A purge tube was added to the setup through which argon was pumped into the cell. If the attraction of oxygen to the surface by the magnetic field is the cause of the shift in the corrosion potential and anodic polarization measurements, then the removal of oxygen from these experiments was expected to remove the variations observed between the samples with and without a magnetic field since oxygen is not present. Each experiment was performed over a five-hour period. Before each experiment, oxygen was displaced from the test cell by pumping argon into the test

cell for 30 minutes. This sometimes results in a shift in each materials initial corrosion potential. No magnetic field was applied during the first three hours of each experiment. After three hours had passed, the magnetic field was turned on and it remained on for the final two hours of the experiment.

It should be noticed in Figure 7, that the corrosion potential never significantly shifted when the magnetic field was applied with the argon environment. These results further confirm that when untreated materials are exposed to a magnetic field in an oxygenated environment, the corrosion potential is shifted due to the increased concentration of oxygen at the surface.

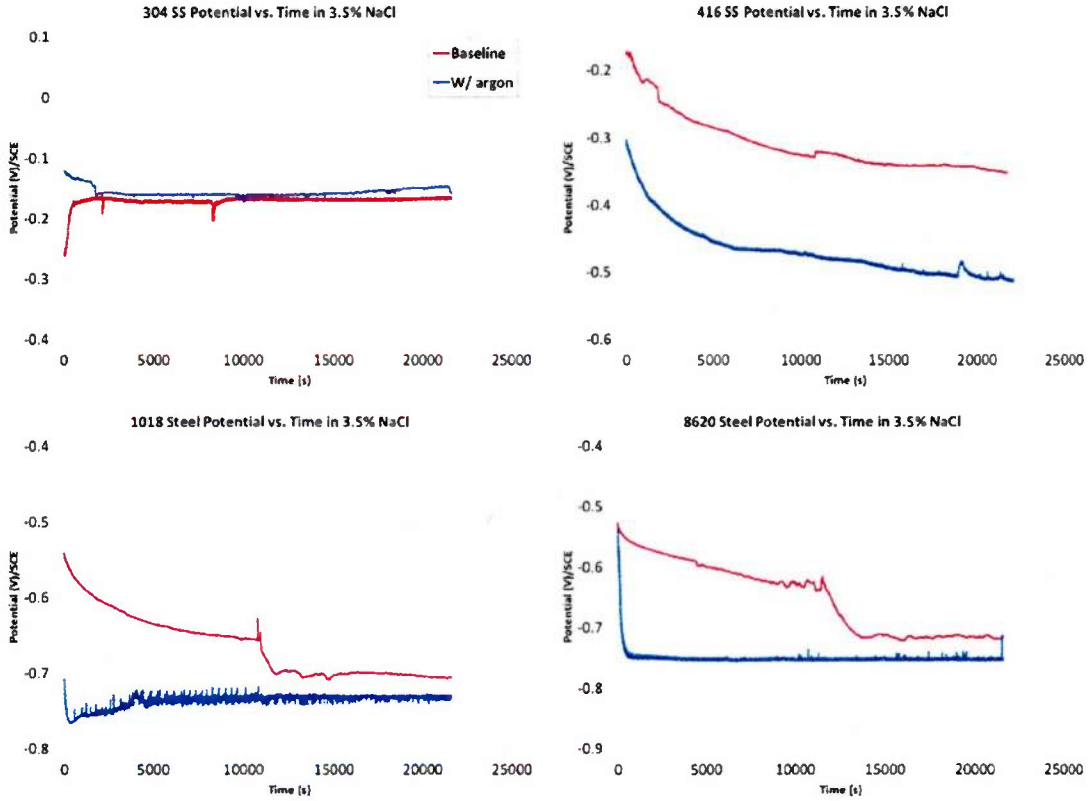

Figure 3. Corrosion potential of 304 SS (top left), 416 SS (top right), 1018 steel (bottom left) and 8620 steel (bottom right) with and without a 0.45 T magnetic field present in argon saturated 3.5% NaCl and an open air NaCl 3.5% NaCl solution (baseline).

The final set of experiments that will be presented are those performed to evaluate how the conduction of high pulsed currents impacts the corrosion rate of the same four metallic alloys tested in the earlier experiments. In all of the experiments performed here, the pulsed power supply is initially charged to 75 VDC. Since the resistivity of the different sample types varies considerably, as seen in Table 1, the resulting current passed through each type of sample varies as well. The 304 and 416 stainless steels have similar resistivity, which are higher than those of either the 1018 steel or 8620 steel. This results in a peak current of roughly 6,500 A being conducted through the 304 stainless steel and 416 stainless steel samples. A peak current of roughly 9,000 A peak is pulsed through the 1018

steel and 8620 steel samples. Current and magnetic field simulations run with each of the different sample types are shown in Figure 8. As seen from the magnetic field simulations, peak magnetic fields ranging from 1.5 T to 3.0 T are generated within the materials under test.

In an effort to understand how the repeated conduction of high-pulsed currents impacts the corrosion rate, each material was pulsed every ten minutes over a three-hour period while submersed in 3.5% NaCl solution. After each material had been pulsed over a three-hour period, linear polarization measurements were made to evaluate the impact the procedure had on the corrosion potential, corrosion current, and polarization resistance. As a means of comparison, the linear polarization measurements were compared to similar measurements made from identical samples, which were only submersed in the 3.5% NaCl solution for three hours without the conduction of current through them. The results are shown in Figure 9. In the case of 304 stainless steel, both the corrosion potential and the polarization resistance increased after exposure to the pulsed currents and magnetic fields. In the case of 416 stainless steel and 1018 steel, both the corrosion potential and the polarization resistance decreased after exposure to the pulsed fields. The corrosion potential of 8620 steel decreased while the polarization resistance increased. The variation in the polarization resistance and corrosion potential between the baseline and pulsed current samples are believed to be a result of the oxygen being influenced by the self induced magnetic field. The dissolved oxygen in the test cell is subjected to the magnetic field altering the oxygen concentration levels on the sample surface. The change in concentration at the surface alters the kinetics of the system changing the corrosion potential and polarization resistance. It is important to note that the kinetics of 304 stainless steel also changed with the applied current pulses. Even though 304 stainless steel is nonmagnetic, a higher self-induced magnetic field alters the kinetics of the sample comparable to the other tested alloys. These unexpected results from 304 stainless steel indicated that it is highly likely that the corrosion properties of most if not all conductors are altered through the conduction of high-pulsed currents.

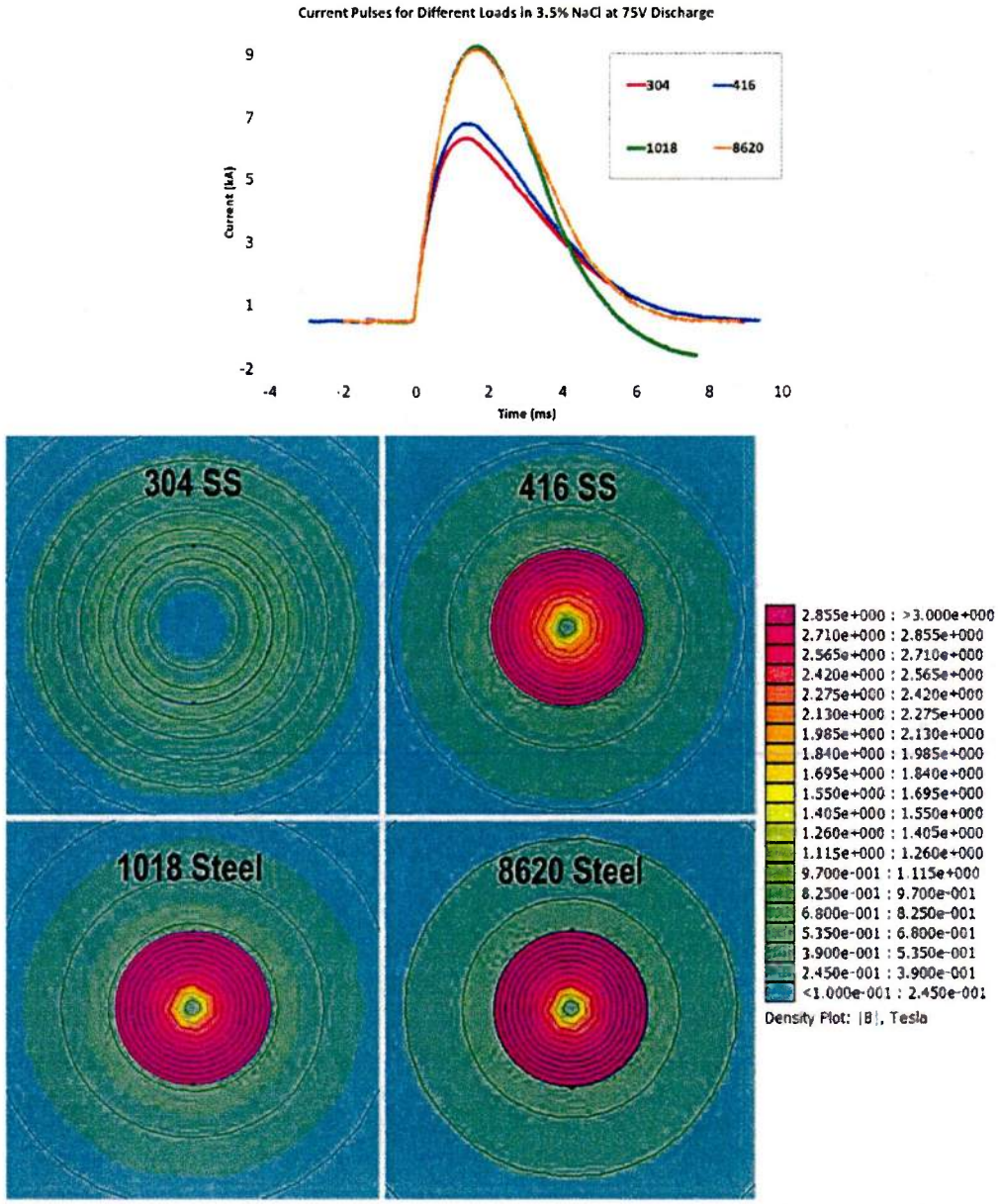

Figure 4. Current sourced by the power supply (above) and magnetic field simulations (below) of 304 SS (top left), 416 SS (top right), and 1018 Steel (bottom left), 8620 steel (bottom right) when pulsed with the currents shown above are applied. Note that the magnetic field simulations assume a sinusoid with a frequency of 111 Hz is applied to the conductor which is approximately equal to the frequency of the applied pulse.

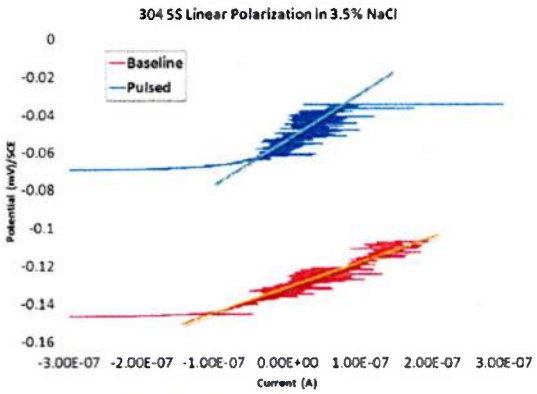

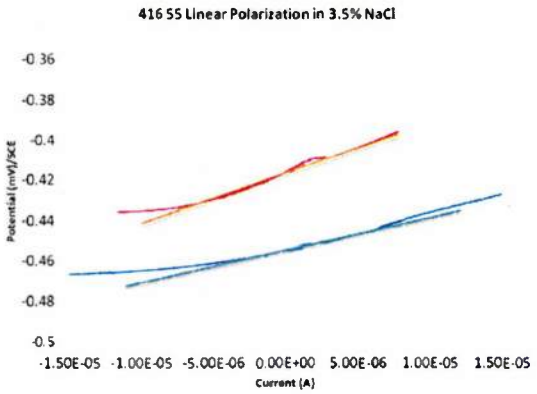

	Corrosion Potential (mV)	Corrosion Current (nA)	Corrosion Resistance (kΩ)
Baseline	-132.1	143.0	152.0
Pulsed	-54.2	78.4	277.4

	Corrosion Potential (mV)	Corrosion Current (uA)	Corrosion Resistance (kΩ)
Baseline	-416.8	7.5	2.9
Pulsed	-459.2	12.1	1.8

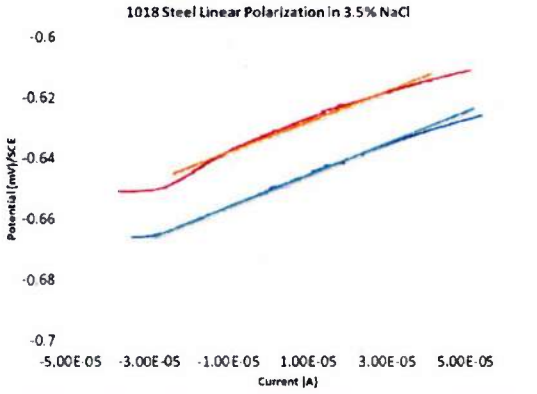

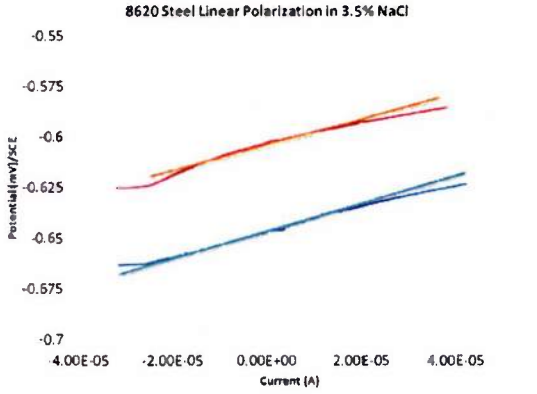

	Corrosion Potential (mV)	Corrosion Current (nA)	Corrosion Resistance (Ω)
Baseline	-632.4	37.4	582.0
Pulsed	-650.7	41.6	536.1

	Corrosion Potential (mV)	Corrosion Current (uA)	Corrosion Resistance (Ω)
Baseline	-603.4	35.9	606.2
Pulsed	-646.8	32.4	671.0

Figure 5. Linear Polarization measurements of 304 SS (top left), 416 SS (top right), 1018 steel (bottom left) and 8620 steel (bottom right) with and without a 0.45 T magnetic field present in argon saturated 3.5% NaCl.

Figure 10 displays SEM images taken of each sample exposed to high-pulsed currents. The 304 stainless steel sample through which current was passed has shallower pits than those on the sample not exposed to current flow. This agrees with the linear polarization results, which show that as current was passed through the sample, the corrosion resistance increased. Therefore, it can be said the 304 stainless steel sample increases its corrosive resistance a high-pulsed field is applied. Remember that when the current was sourced through the 416 stainless steel sample the polarization resistance decreased. When the linear polarization results and SEM image from the 416 sample are compared, it is confirmed that the corrosion resistance had deteriorated since the pitting depth and pitting density increased when compared to that observed on the baseline sample. This is surprising since 416 stainless steel has a relatively high percentage of chromium in

it, which normally results in the formation of a strong oxidation layer. It was expected that the magnetic field would help the 416 stainless steel sample to passivate and protect the alloy, but it seem that the magnetic field helped fuel the corrosion reactions and did not allow the alloy to passivate. The pits imaged on the 1018 steel sample subjected to the pulsed current are deeper than those observed on the sample that did not have current pulsed through it but the pitting density does not appear to have changed between the two samples. Finally, it should be noticed that the pits imaged on the 8620 steel samples that was subjected to a magnetic field are similar in density but shallower than those measured on the sample that did not carry current. Remember that the 8620 steel sample's polarization resistance increased as a result of current flow thereby decreasing the reaction rate and preventing deeper pits from forming.

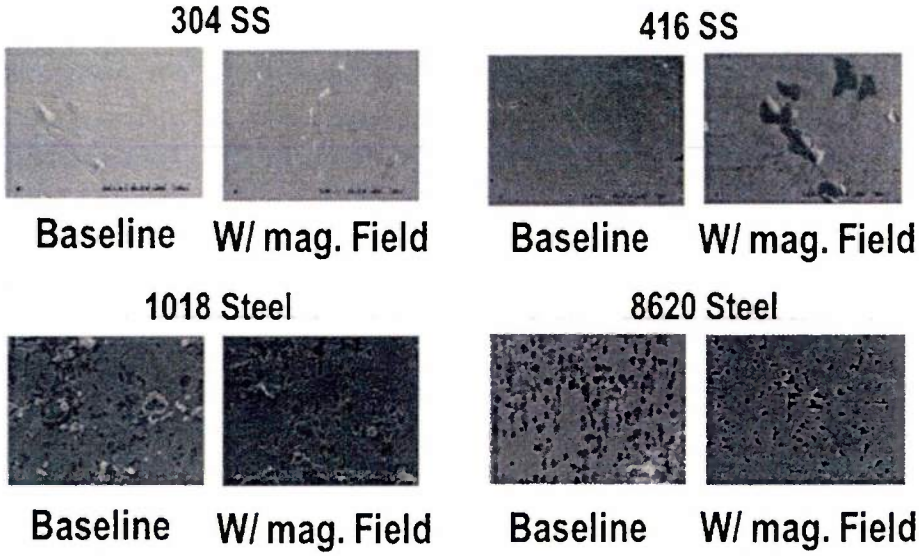

Figure 6. SEM and photographs of the samples measured in Figure 9.

Conclusion

The results produced by the work supported through this grant show that both high pulsed and continuous magnetic fields activate the corrosion reactions, corrosion potentials and kinetics of all materials tested with a more dramatic effect on the 1018 and 8620 steel. Small effects were also observed in 416 and 304 stainless steel. The present results indicate that oxygen plays a major role in the corrosion process when a magnetic field is present. It has yet to be determined whether the change in oxygen concentration is affecting the passivity of the alloys, the cathodic reaction, or both. It has been shown that 304 stainless steel does not appear to be noticeably influenced by an external magnetic field, but is influenced when the magnetic field is self-induced by a high-pulsed current. It is not clear yet if this behavior is due to its inherent passive nature due to high chromium content or due to the fact that it is not ferromagnetic. However, a lower passive current density and lower pitting potential were also observed in 304 stainless steel. The present results clearly

show that the presence of a magnetic field can alter the corrosion process for the four tested materials.

References

1. P. Linhardt et al., "Electrochemical investigation of chloride induced pitting of stainless steel under the influence of a magnetic field," in *Corrosion Science*. Volume 47 (Issue 7), p.1599-1603.
2. P. Linhardt et al. *Pitting of stainless steel under the influence of a magnetic field* [online]. http://info.tuwien.ac.at/cta/korrosion/forschung/magnet.html, December 27, 2012.
3. P. Linhardt et al., "Electrochemical investigation of chloride induced pitting of stainless steel under the influence of a magnetic field," Proceedings of the 4th Kurt Schwabe Symposium Mechanisms of Corrosion and Corrosion Prevention, Helsinki University of Technology, Finland, June 13-18 2004, p. 42-49.
4. M.A. Ghabashy, "Effect of magnetic field on the rate of steel corrosion in aqueous solutions." *Anti-Corrosion Methods and Materials*. Volume 35 (Issue 1), p. 12 – 13.
5. A. Sato et al., "Influence of high magnetic field on the corrosion of carbon steel," *Applied Superconductivity, IEEE Transactions on*. Volume 12 (Issue 1), p. 997 - 1000.
6. *Corrosion in magnetic fields* [online]. http://www.ifw-dresden.de/institutes/ikm/organisation/dep-33/corrosion-in-magnetic-fields, December 27, 2012.
7. R. Pietrzak and R. Szatanik, "Effect of magnetic field on the corrosion of iron as studied by positron annihilation," *Nukleonika 2010*. Volume 55 (Issue 1), p. 31−34.
8. J. Hu at al., "Effects of Applied Magnetic Field on Corrosion of Beryllium Copper in NaCl Solution," *J. Mater. Sci. Technol. 2010*, Volume 26 (Issue 4), p. 355-361.
9. A.J. Davenport and Y.C. Tang, "Magnetic Field Effects in Artificial Corrosion Pits," *J. Electrochem. Soc. 2007*, Volume 154 (Issue 7), p. C362-C370.
10. *Corrosion Costs* [online]. http://www.galvanizeit.org/online-seminar/the-corrosion-problem/corrosion-costs, August 28, 2013.
11. Matweb Materials Property Database [online]. http://matweb.com/, Copyright 1996-2014 by MatWeb, LLC.

Students Supported

1. Clint Gnegy-Davidson (Direct PH.D. Student in Electrical Engineering)
2. Soundarya Pondichery (Masters Student in Material Science)

Papers Written

No papers were published however once conference paper has recently been submitted to the 2014 ASNE MegaRust Conference and two journal papers are in the process of being written

Presentations Given

1. 'Influence of High Pulsed and Continuous Magnetic Fields on the Corrosion and Microstructure of Metallic Conductors,' Naval Surface Warfare Center, Dahlgren Virginia, December 11, 2013.

Acknowledgments

The authors wish to express sincere gratitude to both the US Office of Naval Research (ONR) and the US Department of Energy (DoE) for their respective financial supports which helped to make this work possible. Any opinions, findings, and conclusions or recommendations expressed in this publication are those of the authors and do not necessarily reflect the views of the US ONR or US DoE.